PROCEEDINGS OF THE SIXTEENTH LUNAR AND PLANETARY SCIENCE CONFERENCE, PART 1
JOURNAL OF GEOPHYSICAL RESEARCH, VOL. 90, SUPPLEMENT, PAGES D163–D174, NOVEMBER 15, 1985

The Martian Dust Storm of Sol 1742

HENRY J. MOORE

U.S. Geological Survey, Menlo Park

After nearly five Earth years on Mars, the Mutch Memorial Station (Viking Lander 1) finally witnessed a local dust storm that eroded trenches, conical piles, and other disturbed surfaces in the sample field and near the lander. The event, called the Dust Storm of Sol 1742, occurred late in the third winter of lander observations between Sols 1728 and 1757. Analyses of tiny new wind tails and movement of materials indicate that the eroding winds were variable but more northeasterly than those that had previously shaped the surface. Pebbly residues and movement of 4–5 mm clods suggest drag velocities or friction speeds of the winds were about 2.2–4.0 m/s. Wind speeds at the height of the meteorology boom (1.6 m) were probably about 40–50 m/s. Much of the observed erosion could have occurred in a few to several tens of seconds, but somewhat longer times are suggested by analogy with the erosion of terrestrial soils. Most of the erosion occurred where preexisting equilibrium conditions of surface configurations and surface material properties had been altered by the lander during landing and during surface-sampler activities, but thin layers of bright fine-grained dust were also removed and redistributed. Surfaces where preexisting equilibrium conditions were unaltered appeared to be uneroded.

INTRODUCTION

Sometime in June, 1981, a local dust storm raged in the vicinity of the Mutch Memorial Station (Viking Lander 1), Chryse Planitia, Mars. It is dubbed the Dust Storm of Sol 1742 because an image of the storm in progress was acquired on Sol 1742 [e.g., Figure 6 in *Arvidson et al*, 1983]. (A sol is a Martian day; lander event days are reckoned in sols from the day of landing, which was Sol 0.) For the first time in nearly five Earth years, significant erosion and redistribution of materials in the sample field of the lander were produced by aeolian processes. Some of the general aspects and effects of this storm have been described and illustrated previously [*Moore*, 1982, 1985*a,b*; *Wall*, 1982; *Guinness et al.*, 1983; *Moore et al.*, 1983; and *Arvidson et al.*, 1983]. This paper (1) illustrates additional surface modifications produced by this storm, (2) cites evidence that the wind driections were more easterly than those inferred for winds that previously eroded the surface, (3) suggests that wind speeds 1.6 m above the surface exceeded 30 m/s and were probably about 40–50 m/s, and (4) comments on erosion rates.

The recent geologic processes and weather conditions at the site after more than three Martian years of observations are characterized by mild aeolian activity punctuated by episodic events [*Arvidson et al.*, 1983] (Figure 1). Global dust storms were observed in the fall and winter of the first year [*Tillman*, 1977; *Ryan and Henry*, 1979; *Tillman et al.*, 1979; *Hess et al.*, 1980]; there was probably a major, or possibly a global, dust storm in the fall of the second year [*Ryan and Sharman*, 1981; *Leovy*, 1981; *Guinness et al.*, 1982; *Colburn and Pollack*, 1983]; there was no global dust storm in the third year; and a global dust storm was in progress in the fall of the fourth year [*Tillman*, 1985] when communications with the lander were lost. At the landing site, tens of microns of bright, red dust gently settle to the surface during global dust storms; this dust is subsequently redistributed by mild winds [*Jones et al.*, 1979; *Guinness et al.*, 1982; *Arvidson et al.*, 1983].

Local dust storms appear to be late winter events. A local dust storm of the first year on Sol 423 [*Ryan et al.*, 1981; *James and Evans*, 1981] caused little or no erosion of the surface materials despite estimated wind speeds of 25–30 m/s at 1.6 m above the surface [*Ryan et al.*, 1981]. The local Dust Storm of Sol 1742 was also a late winter event, but it substantially eroded the surface and modified the topography of the sample field. Erosion and modification of materials and surfaces were confined chiefly, if not entirely, to areas where the extant surface configurations and materials had been altered by the lander during landing and during surface-sampler activities.

Six types of surface materials [*Moore et al.*, 1982, 1979, 1977] were exposed to the Dust Storm of Sol 1742: (1) drift material, (2) disturbed drift material, (3) blocky material, (4) disturbed blocky material, (5) dust deposited during global dust storms, and (6) rocks. Undisturbed drift material is a low density soillike material. It is a very fine-grained, cohesive and cross-laminated material. A thin, weak crust is present at the surface. Individual grains appear to be in the clay-size range. Bulk densities are about 1200 kg/m^3, cohesions are about 1.0 kPa, and angles of internal friction are about 20°. The cross-laminations suggest planes of weakness are present. Where disturbed, drift material forms weak lumps and fine materials with very small cohesions. Blocky material is soillike and owes its name to the blocky clods at the ends of trenches in it. Bulk densities are about 1600 ± 400 kg/m^3, cohesions are about 2–16 kPa, and angles of internal friction are about 30°. Disturbed blocky material is composed of tabular to irregular clods (up to 8 cm across), coarse (0.2–1.2 cm) coherent fragments, and finer materials. The sizes of individual mineral grains within the fragments and clods are unknown. Layers of bright dust deposited from global dust storms are tens of microns thick, composed of clay-size grains and appear to have very small to no cohesions. There are a variety of rocks on the surface [*Garvin et al.*, 1981; *Sharp and Malin*, 1984] with essentially unknown mechanical properties. The rocks are as wide as 22 cm in the sample field. They do not chip, scratch, or spall when pushed or scraped by the surface sampler and are much stronger than either drift or blocky materials.

The responses of the various surface materials to engine-exhaust gases during landing were different [*Hutton et al.*, 1980 *Moore et al.*, 1979]. Drift material was not extensively eroded and behaved like a material with a grain size typically smaller than 3–9 μm. Blocky material eroded like a cohesionless fine

Paper number 5B7022.

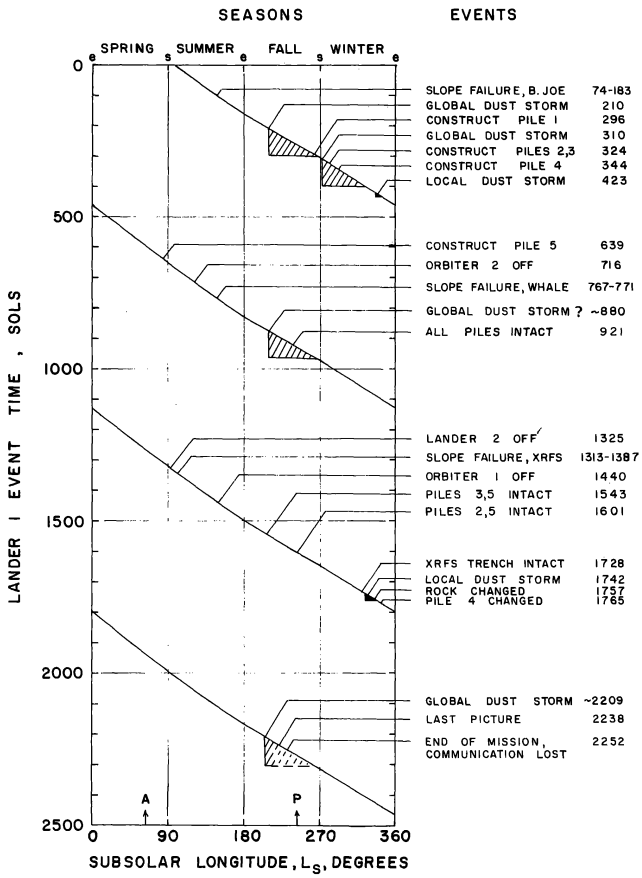

Fig. 1. A chart for all seasons, sols, and some events. Diagonal lines correlate lander event times (reckoned from the time of landing in sols or Martian days) with subsolar longitudinal and Martian seasons. Vertical lines correspond to solstices (s) and equinoxes (e). Sol 0 is the sol of landing (July 20, 1976); Sol 2252 corresponds to the time when communications were lost and is considered here to be the end of the mission (November 19, 1982). The last meteorology and engineering data were acquired on Sol 2256. Selected events are indicated on the right side of the chart. Note that global dust storms occur in the fall and early winter. Local dust storms are late-winter events. The letter "A" indicates the subsolar longitude of aphelion and "P" indicates perihelion.

sand, although it is clearly not sand. Erosion of blocky material produced a rimmed craterlike depression and the debris was deposited in the sample field. Individual rocks up to 7 cm across, 0.8 m from the engine, were moved completely from their original positions, and rocks or clods 2.2 m and beyond may also have been moved by the exhaust gases. In addition, fines and droppings of disturbed drift and blocky materials from the sampler were added to the sample field during surface-sampler activities.

With the exception of the deposition, removal, and redistribution of bright fines from global dust storms, there was no evidence for siginificant changes of trench walls and tailings (the disturbed materials of the rims around the trenches) that could be attributed to Martian winds through the primary, extended, and most of the continuation missions [*Moore et al.*, 1979]. Three conical piles of surface materials, constructed by the sampler, appeared unscathed on Sols 1543 and 1601. Erosion of a fourth pile was first noted in a picture taken on Sol 1765 [*Moore*, 1982]. Subsequent analyses showed that the Dust Storm of Sol 1742 must have occurred between Sols 1720 and 1757 [*Arvidson et al.*, 1983]. The interval may be further constrained between Sols 1728 and 1757, because a high-resolution image of one trench shows that it was unmodified on Sol 1728 [*Moore*, 1985*a,b*]. Finally, a picture of the storm in progress was obtained on Sol 1742. Changes due to the storm are described in the following section.

Observed Changes

Most of the images used to monitor the landing site during the automatic mission were low-resolution images (Table 1; Figure 2). Although the lander was programmed to acquire the images of the same scene systematically [*Arvidson et al.*, 1983], not all of them were received on Earth for a variety of engineering and logisitical reasons [*Wall and Ashmore*, 1985], among which was the lack of availability of radio receivers on Earth. The observed changes will be described in a clockwise direction starting from footpad 2, because the materials change from drift material to blocky material in a systematic way.

Footpad 2

Footpad 2 (area A in Figure 2) became completely immersed in drift material during landing. The drift material was disturbed and deformed to distances of more than 45 cm from the footpad center, producing a depressed surface encircled by a low rim and a scarp 45 cm from the footpad centerline. Another circular scarp, within the depression and later accentuated by slumping and collapse of material, delineated the buried perimeter of the footpad. The relief of the scarp was near 2 cm. In the prestorm image (Figure 3), the disturbed drift material within the footpad perimeter consists of fines and rounded lumps up to 1 cm across. Between the footpad perimeter and the outer scarp, thin platy fragments of surface crust and lumps from the limit of resolution up to 3 cm across are present. In some places beyond the outer scarp, the surface has small sinuous concentric ridges a fraction of a centimeter wide; in other places there is a mosaic pattern produced by fractures.

Comparison or pre- and poststorm images reveals substantial changes (Figure 3*a,b*). The vast majority of the platy fragments and lumps have been destroyed and removed, the originally crisp topographic expressions of the scarps are markedly subdued or obliterated, and the sinuous ridges are altered. The elevation of part of the low rim has decreased locally and the entire low rim is rounded. Lumps about 2 cm thick along the footpad-perimeter scarp are buried by fine material and local slopes are substantially reduced except along a 4 cm segment.

Sandy Flats

Sandy Flats (area B in Figure 2) is the site of many surface-sampler activities (Figure 4*a*), including the excavation of numerous sample trenches in drift material, several backhoe trenches, a surface-bearing test, and an endeavor to scratch rock 2 (Sponge). When rock 2 rolled over toward the lander, a steep face of drift material in the wind tail behind rock 2 was exposed.

In a prestorm low-resolution image (Figure 4*a*), the walls of trenches are steep, their edges and rims are sharp and crisp, lumps within them are evident, and their tailings are clearly discernible. In the poststorm image (Figure 4*b*), most trenches are partly filled with fine material, their edges and rims are

TABLE 1. Images Showing Changes Produced by Dust Storm of Sol 1742

Area shown in images	Post-Storm Type	Post-Storm Frame #	Post-Storm Sol of Image	Pre-Storm Type	Pre-Storm Frame #	Pre-Storm Sol of Image	Observations and Interpretations
A. Footpad 2	Surv.	11J161	1994	Surv.	11J071	1328	Relief of outer scarp reduced; plates of crust and lumps destroyed and removed; rimlike area rounded. Inner scarp partly filled; lumps and plates of crust between scarps eroded.
B. Sandy Flats Trenches; Small Pits; Sponge Wind tail	Surv.	11J166	2031	Surv. BB-2	11J067 1J125	1365 1728	Trench rims rounded; trenches locally filled. Exposed face of wind tail rounded; crestline retreated 6–9 cm. Small pits and depressions rounded and filled. XRFS-7 trench uneroded as of Sol 1728.
C. Conical Pile 4	BB-2	11J130	1765	BB-2 Surv.	11J007 11J080	921 1395	Pile eroded, exposing west side of ventifact; material movement suggests easterly eroding wind; 4–5 mm clods removed; surface roughened by removal of fines.
D. Area Near Lander	Surv.	11J170	2061	Surv.	11J080	1395	Relief of pits, troughs, and ridges near lander reduced by erosion and filling.
E. Rocky Flats, East Conical Piles 2,3,5; Area of Rock 4 Push; Backhoe Trenches 6,8,9	Surv.	11J171	2068	Surv.	11J081	1402	Conical piles 2 and 3 destroyed; relief of pile 5 reduced. Rock 4 disturbed area brightened. Backhoe trenches partly filled and tailings eroded. Relief near lander reduced by erosion and filling; crust and rocks exposed.
F. Rocky Flats, East Conical Piles 2,3,5; Area of Rock 4 Push; Alpha Crater	BB-3	11J190	2209	BB-3 BB-3 BB-2	12J108 11J100 11J103	1601 1543 921	Pile 3 removed; pile 5 eroded to lumpy mound; fines of pile 2 removed from side of rock 3. Fines removed from blocks in disturbed area; clods reduced; perched rock or clod rotated. Crater "alpha" eroded and partly filled; erosion and newly formed wind tails suggest northeasterly wind.
G. Engine Exhaust Crater	BB-1	12J173	2082	BB-1	12D044 12I192	282 836	Relief of rim reduced; slope of wall reduced by filling and erosion; new wind tails on floor; fines deposited at base of nearby rock.
H. Rocky Flats	Color	12J129	1757	Color	12J124	1720	Triangular rock or clod acquired wind tail or flipped over toward west. Excavation in deep hole tailings partly eroded.
I. Rocky Flat, West XRFS-15 Trench Area of Rock 5 Push	Color	12J153	1934	Color	12J063	1268	Trench rims rounded; depressions partly filled; clods destroyed.
J. Edges of Sample Field XRFS-9,11 Trenches, Shroud Impact Crater, Footpad 3	Surv.	12J178	2119	Color	12G229 12I021	542 652	Trench rims eroded leaving residue of clods or rocks, but rim remains peaked; trench floors partly filled; clods to 8 cm reduced and covered. Shroud impact crater eroded and filled. Materials in footpad changed; fines generally removed.
K. Lander Grid, Camera 1	Color	11J160	1987	Color	11J070	1321	Fines moved; part of grid and area to right of grid covered.
L. Lander Grid, Camera 2	Color	12J158	1971	Color	11J068	1305	Fines moved; right corner of grid covered.
M. Big Joe Sky	Color	11J122	1705	Color	11J142	1853	Frame 11J127 (taken on Sol 1742) showed storm in progress; scene darkened; in contrast with prestorm and poststorm images, relative brightness of sky increased upward.

"Type" refers to image resolution. Low-resolution images are Survey (Surv.) and Color. High-resolution images are broad band (BB-2 or BB-3).

rounded, clods and lumps within them are no longer evident, and some tailings boundaries can scarcely be located. These changes are well illustrated by the surface-bearing test trench; originally crisp, raised rims are now bright and rounded and all but the coarsest lumps on the floor are buried. The trench in the wind tail shows similar changes. The pristine form that existed on Sol 1728 no longer exists. The exposed triangular face of the wind tail that adjoined rock 2 exhibits a substantial change. This initially concave, steeply sloping surface, with 5 cm of relief, had survived for more than 887 sols. After the storm, the face became convex and rounded; the leading crest of the wind tail, originally marked by a small fragment, migrated 6–9 cm along the crest in a southerly direction. Crude estimates suggest that 100–200 g of material were eroded away.

Elsewhere, subtle sinuous ridges were rounded or destroyed; small grooves and elongated impact pits were filled with or buried by fine material. In some places, dark bands and patterns replaced initially bland surfaces.

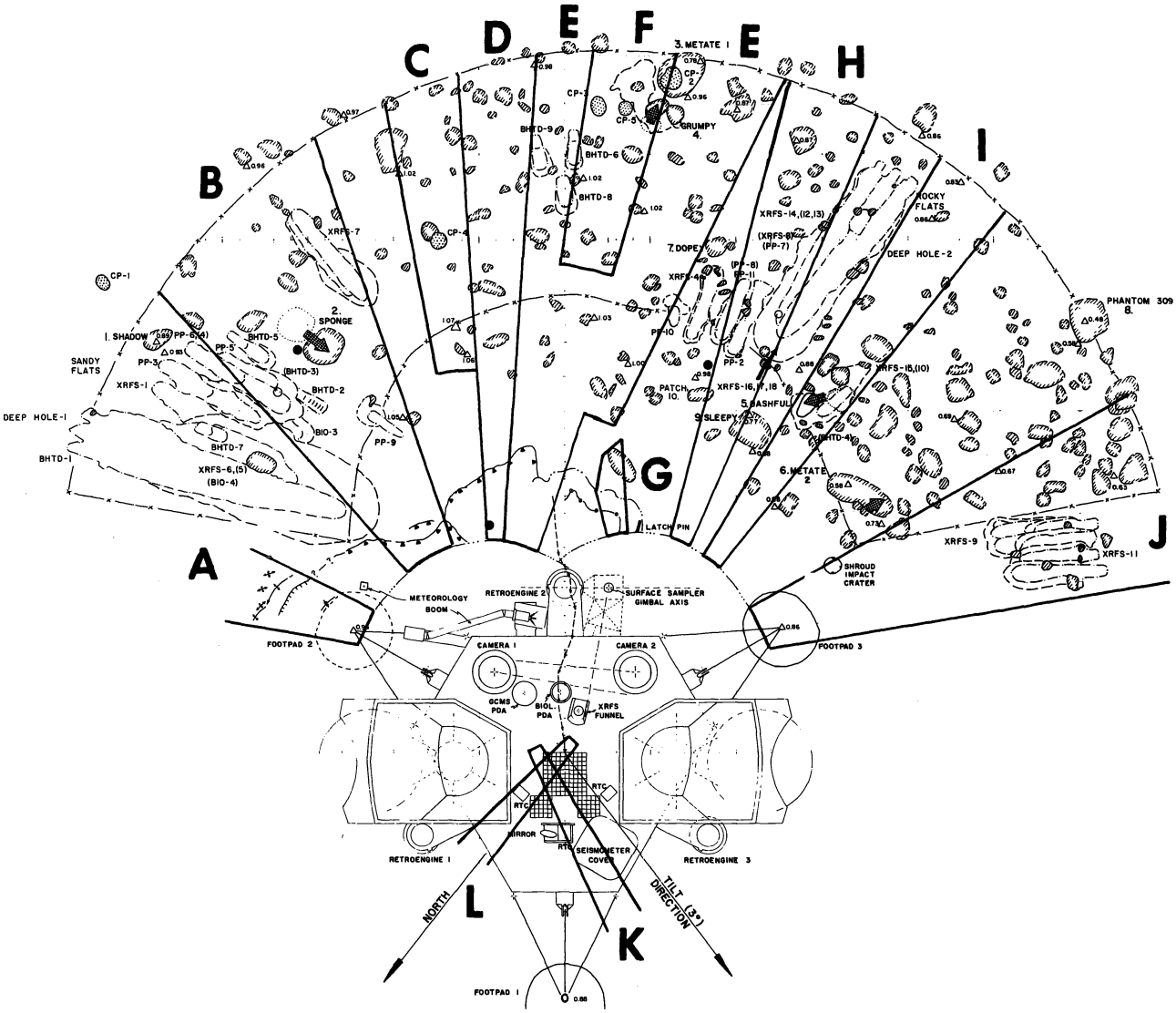

Fig. 2. Planview of Viking Lander 1 and sample field showing areas covered by images taken after the Dust Storm of Sol 1742. Letters correspond to entries in Table 1 and in text. Trench rims are outlined by dot-dash lines; rocks indicated with diagonal hachures; conical piles (CP-1-5) indicated with dot pattern [after *Moore and Dowey*, 1981].

Conical Pile 4

Conical pile 4 (area C in Figure 2), which partly covered the western side of a rock 7 cm tall with disturbed drift material (Figure 5*a,b*), provides information on the direction of the wind that eroded the pile [*Moore*, 1982]. The poststorm image reveals that the originally covered western side of the rock is exposed, and a fragment of the western base of the pile is completely buried by material blown from the pile. Fragments at the northwestern and southwestern base of the pile are exposed or partially buried. Thus the eroding winds came from an easterly direction.

Nearby, a pile of 4–5 mm fragments (Figure 5) that were present before the storm are missing the poststorm image. Removal of the fragments may have been due to direct entrainment in the wind, or they may have been eroded by the impact of finer grains entrained in the wind. Additionally, the poststorm surfaces are stripped of the preexisting bright, fine materials deposited by global dust storms, engine-exhaust gases, and the surface sampler.

Area Near Lander

The area near the lander (area D in Figure 2) does not include any trenches or piles. Poststorm coverage is a partial low-resolution image 7.2° wide that shows that the foreground is underlain by drift material. In the prestorm image the foreground has shallow troughs, pits, and a random array of small clods dropped from the sampler and deposited from engine-exhaust gases. In the poststorm image the troughs, pits, and most of the small clods are gone.

Rocky Flats, East

Rocky Flats (East) (areas E and F in Figure 2) includes three backhoe trenches, three conical piles, an area disrupted during a rock push (rock 4, Grumpy), a crater ("alpha") related to engine-exhaust erosion, and part of a surface-bearing test trench (area E in Figure 2). Blocky material underlies the surface of Rocky Flats (East), except in the foreground where there is a thin layer of drift material and superposed deposits from

engine-exhaust gases and surface-sampler activities. The foreground is ridged, grooved, pitted, littered with small clods, and dotted with partly buried rocks. Most of the poststorm coverage is low resolution, but a high-resolution image covers important parts of the area (area F in Figure 2). The prestorm low-resolution image (Figure 6*a*) shows the following: (1) The three backhoe trenches are still deep with sharp edges and raised rims, and they retain their tailings of fine material, clods, and small rocks. (2) All three conical piles rise majestically 3 to 4 cm above their surroundings. (3) The disrupted area around rock 4, crater "alpha," and the tip of the surface-bearing trench appear unchanged. (4) The ridged, grooved, pitted, littered, and rock-dotted foreground appears much the same as in previous images. The poststorm low-resolution image (Figure 6*b*) shows the following: (1) The three backhoe trenches are difficult to locate because they are partly filled, their rims eroded, and the only remnants of their tailings are scattered clods and rocks. (2) Conical pile 2 (atop rock 3) and pile 3 (among rocks) are gone; all that remains of pile 5 is a rounded mound. (3) Clods within the disturbed area appear brighter than before, and two bright objects, probably rocks, are exposed at the base of rock 4. (4) The shape of crater "alpha" is changed. (5) A residue of clods and rocks remains at the tip of the surface-bearing test trench. (6) In the foreground, ridges are rounded or destroyed, grooves and pits filled, many clods buried, moved, or destroyed, and buried rocks are exhumed; in some areas, new mosaic patterns suggest the presence of newly exposed crust.

High-resolution images of part of Rocky Flats (East) reveal changes at a level of detail not possible with the low-resolution images. The prestorm image (Figure 7*a*) shows that conical piles 3 and 5 were indeed conical. The poststorm image (Figure 7*b*) shows that pile 3 is gone, although a dozen or so lumps of material are present where it once stood. Alterations of pile 5 are different than pile 3, because pile 5 was constructed with blocky material and pile 3 was constructed with drift material. In contrast with pile 3, which was leveled, pile 5 is a broad mound with coarse fragments up to 0.7 cm wide. The relief of the pile was reduced 0.9–1.4 cm and the base expanded in a southwesterly direction.

Fig. 4. Prestorm (*a*) and poststorm (*b*) images of Sandy Flats. Note the following changes from (*a*) to (*b*): (1) Trenches (b and t) are partly filled and rims are rounded; (2) trench (x), which was uneroded on Sol 1728, is partly filled and rims are rounded; (3) bright fine materials are removed from rock 2 (s); (4) triangular face (w) of wind tail originally behind rock 2 (s) is rounded and the peak of the crest has retreated 6–9 cm; (5) impact pit (p) has disappeared; and (6) ridges of foreground are rounded and depressions are filled with fine material. Sun is from right. Scenes correspond to (B) in Figure 2 and Table 1. (Frames 11J076/1365 and 11J166/2031.)

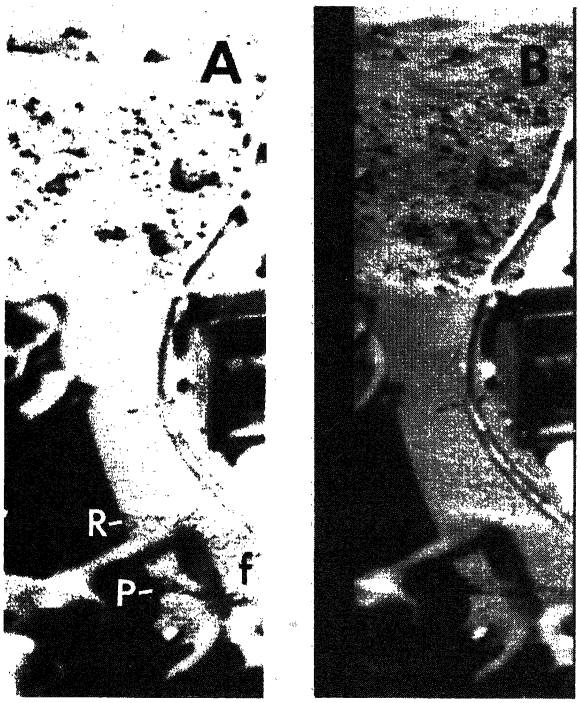

Fig. 3. Prestorm (*a*) and poststorm (*b*) images of surfaces above footpad 2. Note the following changes from (*a*) to (*b*): (1) Low rim (R) is rounded; (2) footpad perimeter scarp (P) is infilled—especially below f; (3) clods and fragile platy fragments between low rim and perimeter scarp are gone—especially above f; and (4) lumps inboard of perimeter scarp appear muted. Sun is from upper right. Scenes correspond to (A) in Figure 2 and Table 1. (Frames 11J071/1328 and 11J161/1994.)

In prestorm images (Figure 7*a*), the disrupted area near rock 4 consists of jumbled blocky clods and possibly rocks, up to 9 cm across and 4 cm thick; the local relief is as high as 5 cm in places. Many of the blocks are topped by layers and piles of fine material and small clods; one block has a 3-cm fragment on it. At the left or eastern edge of the disrupted area, coarse lumps, clods, and fine materials form a mound with about 0.5 cm of relief. Between rock 4 and the larger blocks, the surface is complicated with clods and locally depressed areas. In the poststorm image (Figure 7*b*), about 1.5 cm of fine material is removed from the easternmost block, and the relief of another pile of fine material is reduced 0.5 cm. Relief of the eastern edge of the disrupted area is 0.5 cm lower that it was before the storm, and clods (as large as 1 or 2 cm) are destroyed. Local deposition of fine material has filled depressions and lows between clods and rocks, especially in the area between the larger blocks and rock 4. Movement of the 3-cm rock perched atop the largest block is interesting because it appears to be rotated and tilted, but not significantly translated. Detailed

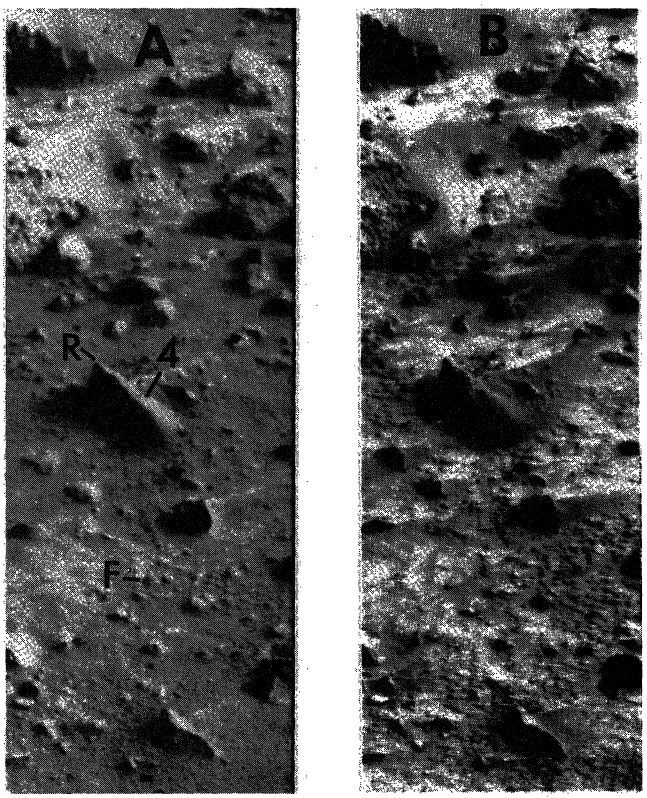

Fig. 5. Prestorm (*a*) and poststorm (*b*) images of conical pile 4. Note the following changes from (*a*) to (*b*): (1) Conical pile (4) is eroded; (2) west side of rock (R) has become exposed; (3) clods at west base of pile are partly to completely buried; (4) small (4–5 mm) fragments (F) are removed; and (5) bright fine materials in foreground and elsewhere are gone. Sun is from right. Scenes correspond to (C) in Figure 2 and Table 1. (Frames 11J007/921 and 11J130/1765.)

mapping shows that it was trapped by a clod or block to the southwest. A northeasterly wind is suggested by removal of material from the northeastern edge of the disrupted area and the easternmost block, deposition of fine materials in more westerly areas, and the entrapment of the perched rock.

Crater "alpha" was produced by either displacement of a rock or impact of debris propelled by engine-exhaust gases during landing (Figure 7*a*). It is about 5.5 cm wide and 12 cm long. Prior to the storm, the crater had rims 0.5–1 cm high, and its planview outline was pear-shaped. In the poststorm image (Figure 7*b*), the rim is absent except for a residue of fragments about 0.5 cm across. The crater is partly filled, especially in the eastern tip, and its southwestern walls are eroded. This filling and erosion have altered its shape. New wind tails are found behind objects on their downwind sides. These new wind tails imply that the wind came from about N 30° E, which is consistent with the deposition in and removal of materials from crater "alpha."

The southwestern edges of two backhoe trenches are visible in the high-resolution images. Changes produced by the dust storm include: (1) deposition of 0.5–0.8 cm of fine material in one trench, (2) removal of fine material from parts of the rims of both trenches, leaving a residue of fragments 0.4–1.6 cm across, (3) total removal of rim segments 0.8 cm high, (4) introduction of fragments 0.4 cm across on the floor of one trench, and (5) displacement of a 1 × 3 cm rock or clod.

Engine-Exhaust Crater

A flat-floored, rimmed crater (area G in Figure 2) was produced by engine-exhaust gases during landing (Figure 8*a*). Scouring by the gases exposed a fractured, planar substrate 0.5 m outward from the engine centerline. Deposition and redistribution of materials resulted in a sinuous raised rim with platy to equidimensional fragments as large as 1 cm imbedded in it. A rock, an impact pit, and more deposited material are located beyond the rim. The poststorm image (Figure 8*b*) shows the following changes: (1) The area of exposed, fractured, planar substrate has increased and changed because of the redistribution of fine material. (2) The slope of the inner wall is reduced by the deposition and redistribution of fine material at its base and erosion near its crest. (3) Scouring has enhanced exposure of some fragments, but some fragments have deposits of fine material as thick as 1 cm on their leeward sides. (4) New wind tails oriented N 17° E are found on the crater floor. (5) Beyond the rim, the impact pit is gone, the surface appears scoured, and a deposit of a dark, fine material is present at the base of the rock. Interpretation of wind speeds with directions of the dust storm here are clouded because the crater is located beneath the lander where wind patterns are complicated.

Rocky Flats

Prestorm images of Rocky Flats (Figure 9*a*) (see area H in Figure 2) include an excavation in the tailings of Deep Hole

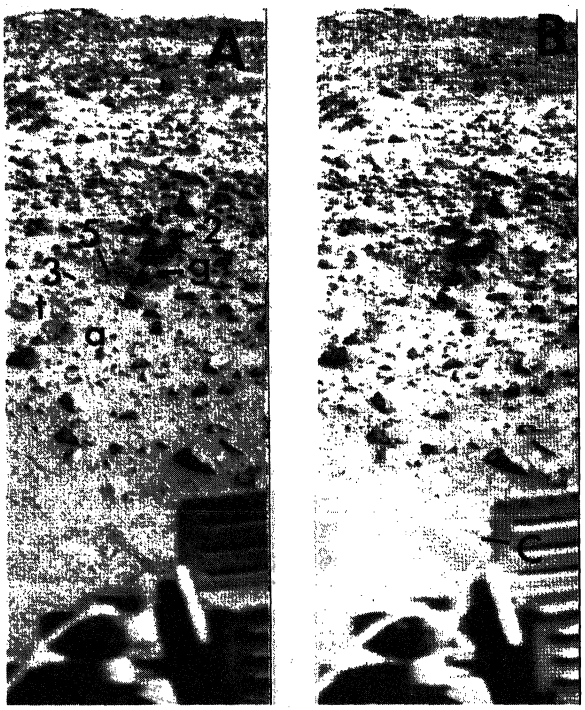

Fig. 6. Prestorm (*a*) and poststorm (*b*) images of Rocky Flats (East). Note the following changes from (*a*) to (*b*): (1) two piles (nos. 2 and 3) are removed; (2) one pile (no. 5) is partly removed; (3) two rocks below rock 4 (g) are exposed; (4) disrupted area to left of rock 4 (g) has brightened and changed; (5) three trenches (around t) are partly filled and their rims are destroyed; (6) shape of crater "alpha" (above a) has changed; and (7) erosion and filling have occurred in foreground (C). Sun is from the right. Scenes correspond to (E) in Figure 2 and Table 1. (Frames 11J081/1402 and 11J171/2068.)

2, the east rim of the tailings of Deep Hole 2, a trench partly filled as a result of previous sampler activities, and the western edge of another trench. All trenches were excavated in blocky material. It should be noted that a segment of the steep inner wall of the excavation in the tailings collapsed before the dust storm sometime between Sols 1313 and 1387. Changes induced by the storm were both erosional and depositional (Figure 9*b*). Some large objects were displaced. In particular, the eastern ridge of the excavation in the deep-hole tailings appears to be narrower and fragments appear to be more obvious than in prestorm images. A northeast-trending ridge, 6 cm long and 1 cm high, on the northern flank of the excavation disappeared along with a nearby rock or clod 3 cm across. The blocky tailings nearest the lander were eroded and crevices were filled; one large rock rotated a small amount. A triangular fragment at the edge of a small trench either has a wind tail deposit on its southwestern side, or it has flipped over toward the southwest; in either case, an easterly wind (N 65° E) is implied. A nearby clod or rock has disappeared and crevices and low areas were filled. Elsewhere in the area, removal of bright, fine materials has exposed small rocks and increased the contrast of preexisting wind tails so that their forms are clear. Near the lander, shallow swales are filled with a dark-colored fine material.

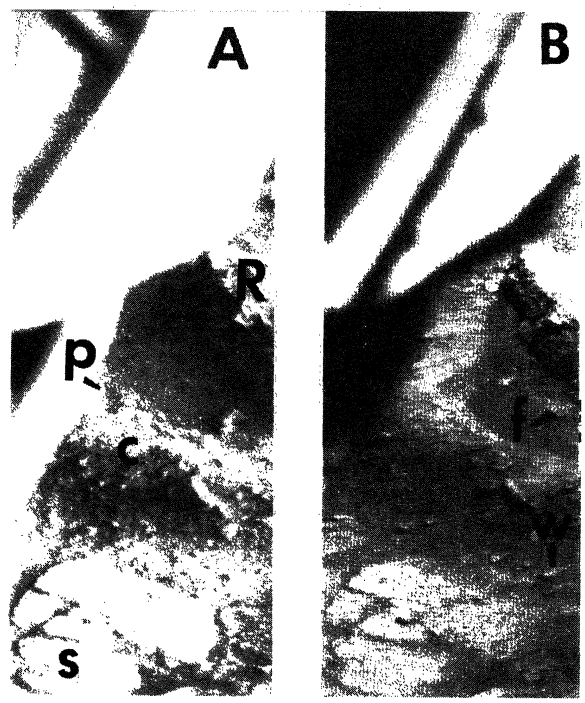

Fig. 8. Prestorm (*a*) and poststorm (*b*) high-resolution images of engine-exhaust erosion crater. Note the following changes from (*a*) to (*b*): (1) Rim crest (c) has been eroded and fines are deposited on slope of wall (below c); (2) pit (p) is gone; (3) a dark, fine material (f) appears at base of rock (R); (4) new wind tails appear (w); and (5) exposures of planar flat floor (s) of crater have changed and increased. Sun is at right (in *a*) and top right (in *b*). Scenes correspond to (G) in Figure 2 and Table 1. (Frames 12D044/282 and 12DJ173/2082.)

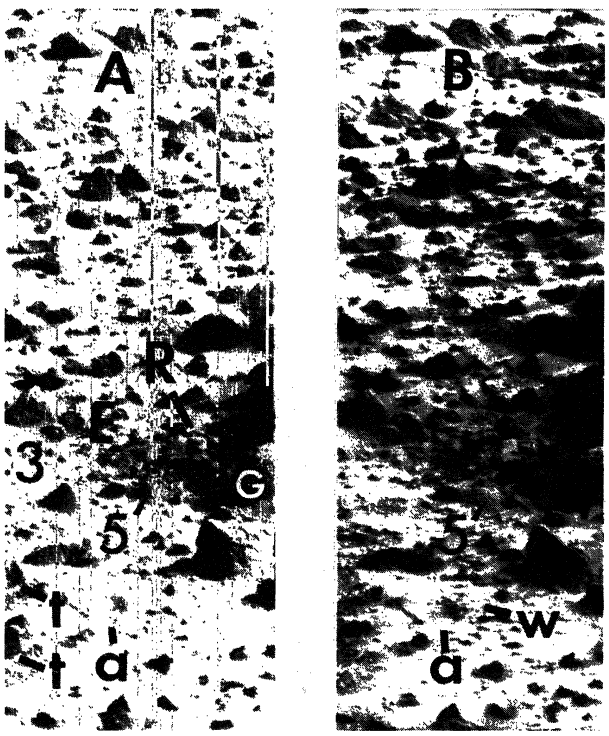

Fig. 7. Prestorm (*a*) and poststorm (*b*) high-resolution images of Rocky Flats (East). Note the following changes from (*a*) to (*b*): (1) rock or clod (R) has rotated; (2) elevation of east part of disrupted area (E) is lower and centimeter-size clods are gone; (3) one pile (no. 3) is gone, but lumpy residue remains; (4) relief of another pile (no. 5) is reduced but a mound of coarse fragments remains; (5) rims of trenches (t) are demolished; (6) shape of crater "alpha" (a) has changed because east side is partly filled and west side is eroded; and (7) new small wind tails (w) have formed behind small fragments on downwind side of crater "alpha." Rock 4 is labeled "G." Sun is from upper right. Scenes correspond to (F) in Figure 2 and Table 1. Vertical lines in (*a*) are missing data. (Frames 11J100/1543 and 11J190/2209.)

Rocky Flats, West

Rocky Flats (West) (area I in Figure 2) includes a rather messy area generated while moving rock 5, a trench in the messy area, and a bright foreground dotted with rocks. In the prestorm image (Figure 10*a*) trench rims, tailings, piles, and ridges of blocky material near displaced rocks are sharp, crisp, and contain abundant clods. The foreground and background are covered by bright, fine materials so that surface contrasts are small. In the poststorm image (Figure 10*b*) trench rims, tailings, piles, and ridges near displaced rocks are rounded, and most of the clods are destroyed or reduced in size. Fine-grained deposits occupy the floor of the trench and other depressions. Newly formed small wind tails that trend about N 30° E are found near the base of a rock. In the foreground, removal of bright, fine materials increases the scene contrast and reveals preexisting wind tails with vivid clarity; locally, dark smooth fines fill shallow depressions and bury objects as large as 1 cm. Scene contrast in the background is greater than that prior to the storm; dark patches probably represent removal of overlying bright dust, but dark deposits are also possbible.

Edge of Sample Field

The edge of the sample field (area J in Figure 2) is covered by low-resolution images that include overlapping trenches in blocky material, the shroud impact crater, and footpad 2. Four overlapping trenches obliterate all but the ends of the tailings

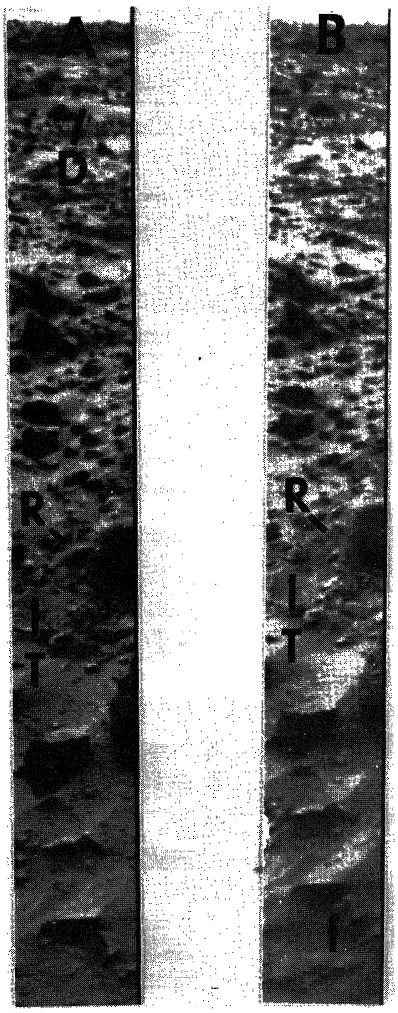

Fig. 9. Prestorm (*a*) and poststorm (*b*) red color images of Rocky Flats. Note the following changes from (*a*) to (*b*): (1) Ridge on tailings (R) has been eroded and reduced; (2) triangular rock (T) has acquired a wind tail or flipped over toward the west; and (3) dark, fine materials (f) appear near rocks in foreground. "Active dune" indicated with "D." Sun is at upper right. Scenes correspond to (H) in Figure 2 and Table 1. (Frames 12J124/1720 and 12J129/1757.)

of three earlier trenches. The trenches, up to 60 cm long, span an area 42 cm wide. Before the storm (Figure 11*a*), interior relief of the trenches is as great as 6 or 7 cm and exterior relief of the tailings is as great as 4 cm. Materials in the trenches consist of rocks up to 9 cm across, blocky clods with a wide range of sizes and shapes, and fine materials. The poststorm image (Figure 11*b*) shows that changes are related to erosion, deposition, and redistribution of materials. Tailings rims are narrower and more pebbly than in prestorm images; trench floors are shallow with U-shaped profiles, whereas they had been deeper and V-shaped. Unusually deep parts of the trenches are completely filled. While some tailings rims are straighter and others more sinuous in poststorm images than in prestorm images, there are no major displacements at right angles to the trench axes. Trench rims are deflated at their far ends, initially steep slopes and scarps are shallow and, in some cases, obliterated, and large blocky clods (up to about 7 cm across with several centimeters of relief) have disappeared. Some of these clods were eroded away, and other were buried by fine materials and small clods. Beyond the trenches and along their axes for about 0.3 m, the surface is dark compared to surrounding surfaces; this darkened surface was not evident before the storm. To the right of the trenches, removal of bright dust has increased the contrast in this initially pebbly area.

These observations are entirely consistent with an eroding wind from the northeast that would place the trenches in the turbulent wake of the lander. Even in a turbulent wake, materials generally move in directions parallel to the prevailing winds. There are no major lateral shifts of the tailings rims, fine materials have accumulated at the far ends of the trenches, and the dark surfaces beyond the trenches are probably thin deposits. Thus the wind came from the northeast.

The obliteration of large blocky clods, subdual and obliteration of initially steep slopes, the coarse pebbly residues, and downwind deposits attest to unusually strong winds and large wind friction speeds.

The shroud impact crater was produced on Sol 2 near footpad 3 by the ejection of rocks, clods, and fine material [*Moore et al.*, 1977]. In the prestorm image (Figure 11*a*), the crater floor is rough, hummocky, ridged, and littered with fragments as much as 1 cm wide. A raised rim with about 0.5 cm relief and fragments as much as 2–3 cm wide encircle the crater. Surrounding surfaces are bright, but littered with numerous millimeter-size fragments (part of which are droppings from the sampler), pitted, and dotted with centimeter-size fragments. The poststorm image

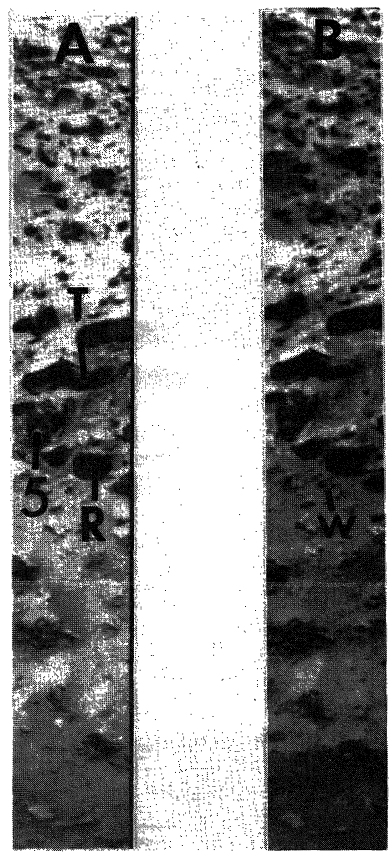

Fig. 10. Prestorm (*a*) and poststorm (*b*) red color images of Rocky Flats (West). Note the following changes from (*a*) to (*b*): (1) Trench (T) is partly filled, its rims are rounded, and some clods are gone; (2) ridges of disturbed material below rock (no. 5) are rounded and clods are gone; (3) new wind tails (w) appear below rock (R), and (4) contrast of foreground has increased. Sun is at top left. Scenes correspond to (I) in Figure 2 and Table 1. (Frames 12J063/1268 and 12J153/1934.)

(Figure 11*b*) shows that there has been substantial filling and erosion. The crater floor is smooth instead of rough, and some of the centimeter-size fragments are buried by a dark, fine-grained material; the raised crater rim is gone, but some large fragments of it remain. Surfaces surrounding the crater are covered with a smooth, dark, fine material that buries the small millimeter-size fragments and pits; only the largest centimer-size fragments are visible.

In footpad 3, the amount and distribution of fine materials have changed often. These materials were initially deposited after they were entrained by engine-exhaust gases. Subsequent changes were the result of wind eddies, surface-sampler activities, and spacecraft vibrations. When last photographed on Sol 921, the distribution of material was essentially the same as that shown as in Figure 11*a*. Comparison of pre- and poststorm images (Figure 11*a,b*) shows the following: (1) A skiff of fines is added to the outer edge of the footpad. (2) Fine materials are removed from the eastern wall along with the addition or redistribution of some material. (3) Fine materials are removed from the southern and western walls. (4) The symmetry of the pattern of materials on the floor has changed. In general, the poststorm image suggests a general depletion of material in the footpad and that darker fines have been added.

Far Field and Other Changes

Changes produced by the storm beyond the sample field are difficult to assess. In the poststorm images, ripplelike bedforms with 4–5-cm wavelengths appeared in several places [*Arvidson et al.*, 1983], but it cannot be established with certainty that they were produced by the storm—they may have been exhumed by the removal of superposed bright materials. In many places, the contrasts of the drift surfaces were enhanced so that surface details became vivdly clear. Judging from changes that occurred in the sample field, the increased contrast could be due to some combination of removal of bright fine materials and deposition of a relativley dark-colored fine material. A bright drift beyond area D (Figure 2) became darker so that two rocks in front of it could no longer be identified. A dune (D in Figure 9) beyond area H was postulated to be active. There is no evidence that it moved; it became darker in blue, green, and red images. The slumps in drift material at the base of Big Joe [*Jones et al.*, 1979] and Whale [*Guinness et al.*, 1982] rocks were not extensively modified; however, they became brighter with time and the original surface details were no longer as vivid as they were prior to the dust storm.

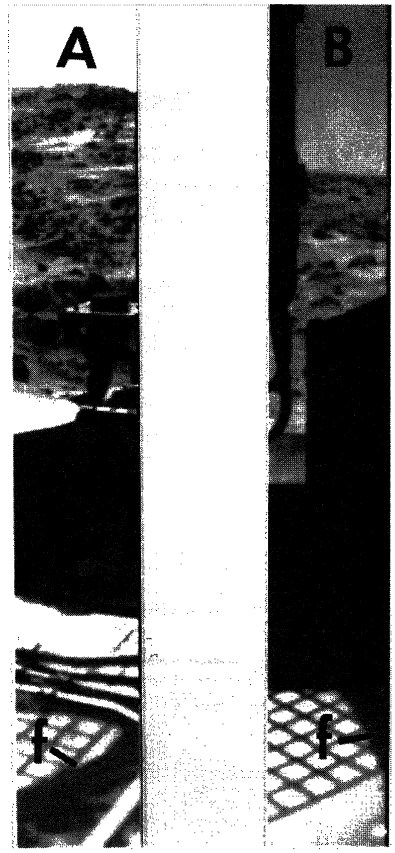

Fig. 12. Poststorm images of grid area taken by cameras 1 and 2. Note fines (f) on east side of lander grid in (*a*) and (*b*). Scenes correspond to (K) and (L) in Figure 2 and Table 1. (Frames 11J160/1987 and 12J158/1971.)

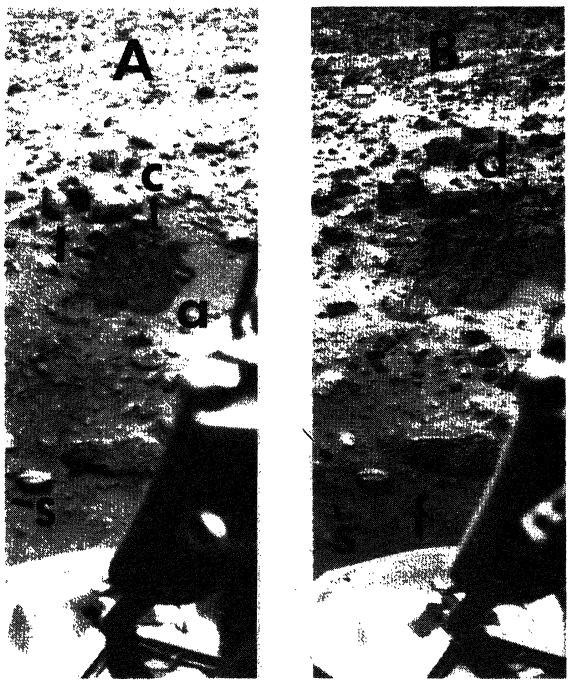

Fig. 11. Prestorm (*a*) and poststorm (*b*) images of edge of sample field. Note the following changes from (*a*) to (*b*): (1) Profiles of trenches (t) have changed from V- and to U-shaped; (2) removal of fine materials from rims has left pebbly residues; (3) far ends of trenches (toward c) are deeply filled; (4) clod (c) and others nearby have disappeared; (5) removal of bright fines (above a) has left dark pebbly residue; (6) dark deposits (d) appear at ends of trenches; (7) shroud impact crater (s) is filled with dark fines and its rim is eroded; (8) dark fines (f) cover clodlets, pits, and rocks; and (9) pattern of deposits in footpad at bottom of images has changed. Scenes correspond to (J) in Figure 2 and Table 1. (Frames 12I021/652 ad 12J178/2119.)

Lander Grid

The grid atop the lander (areas K and L in Figure 2) had material dumped on it many times throughout the primary and extended missions; the distribution and amount of material have changed continually because of wind eddies, sampler activities, and spacecraft vibrations. Although the relevance is unclear and image coverage is sparse, it appears that some materials on the grid are concentrated on the east side of the grid area in poststorm images (Figure 12*a,b*) where none was present before.

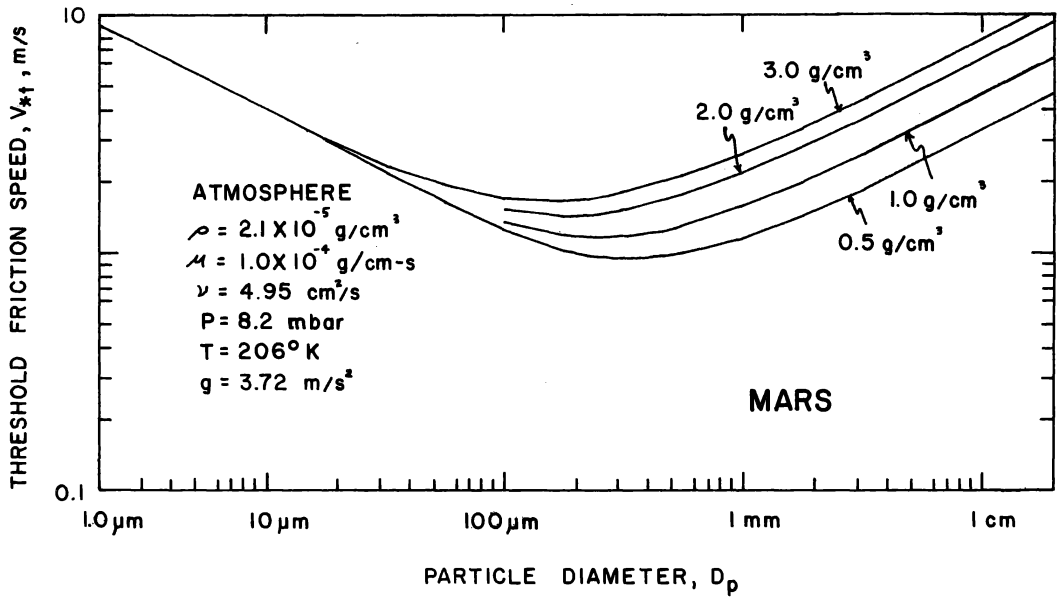

Fig. 13. Threshold friction speeds and particle size for four particle densities and atmospheric conditions that prevailed during the Dust Storm of Sol 1742. Symbol "g" is acceleration of gravity. Symbols for atmosphere properties the following: density (ρ), viscosity (μ), kinematic viscosity (ν), pressure (P), and temperature (T).

Perhaps wind tunnel simulations will reveal the significance of this observation.

INTERPRETATIONS

In order for surface erosion to occur, surface topography and the mechanical properties of the surface materials present must be in a condition of disequilibrium with respect to the stresses exerted by the wind and its entrained debris. The erosion was associated with surfaces disturbed during landing, trenches excavated by the sampler, conical piles constructed to detect and measure wind erosion, and other artificial modifications. Elsewhere, thin bright deposits from global dust storms were stripped from dunes, drifts, and rock surfaces.

In order to saltate and entrain particles, wind stresses or drag velocities must exceed a certain value [*Bagnold*, 1941] called the threshold friction speed [*Iverson et al.*, 1976*a,b*]. Extensive wind tunnel experiments have been conducted to establish the relationship between threshold friction speeds and particle size under conditions that simulate the Martian atmosphere [*Iverson et al.*, 1976*a,b*]. The effect of differences in accelerations of gravity for the Earth and Mars are resolved with well-known principles of dimensional analyses and physics. The effects of interparticle forces have been partially assessed with theory [*Iverson et al.*, 1976*a*]. There are several shortcomings in the wind tunnel tests and theory that are not fully assessed, such as the role of interparticle forces and cohesion, although it is clear that cohesionless particles are more easily moved. More importantly, the surface materials of Mars are complex with a wide range of physical properties and particle sizes; the wind tunnel tests and theory deal with rather simple, homogeneous materials. According to equations (1) and (2) of *Iverson et al.* [1976*b*], which are used in calculations below, threshold friction speeds depend on the size and density of the particle, the density and viscosity of the atmosphere, and the acceleration of gravity of Mars. In turn, the density and viscosity depend on atmospheric pressure and temperature. Solutions to the equations mentioned above for threshold friction speeds of particles with diameters of 1 μm to 2 cm, densities of 0.5 to 3.0 g/cm^3, and the values for atmospheric properties appropriate for the late winter season on Mars are shown in Figure 13.

Depending on particle density, there is a particle size corresponding to a threshold friction speed required to saltate or entrain the particle; there is also a particle size corresponding to a minimum threshold friction speed. For wind friction speeds greater than this minimum, particles between the appropriate threshold friction speeds will be set in motion if they are present and are exposed to the wind. The larger ones may move by surface creep or saltate, and the smaller ones may become suspended in the wind. Once the entrainment process begins, the impacts of saltating and suspended particles with other surfaces set ever increasing numbers of particles in motion. Saltating and suspended particles will also erode clods and rocks to varying degrees depending on their speeds, strengths, and the mechanical properties of the impacted objects.

The changes produced by the dust storm can be interpreted in a variety of ways that depend on assumed values used in calculations and the model employed to account for the changes. In one model, one may assume that erosion was produced by small particles entrained in the wind. In this case, threshold friction speeds need only be high enough to set an optimum particle size in motion by saltation. Particles finer than this minimum size are dislodged by the impact of saltating particles and suspended in the atmosphere. Clods are reduced or destroyed by the impacts of saltating and suspended particles. Erosion by impact and abrasion most certainly occurred because large cohesive clods, much too large to move, were reduced and destroyed. Minimum threshold friction speeds for plausible particle densities (1.0–3.0 g/cm^3) are 1.2–1.7 m/s and correspond to particle sizes of 250–180 μm. *Sutton et al.* [1978] suggest that surface roughness heights between 0.1 and 1.0 cm are reasonable for the Viking site. From the Prandtl-Von Karman equation [e.g., equation (9) in *Iversen et al.*, 1976*a*], wind speeds at the height of lander's on-board wind sensor (1.6 m) need

only have been 15–22 and 21–32 m/s for the surface roughness heights above. This interpretation appears unlikely because the winds of the local dust storm of Sol 423, which did not erode the sample field, were estimated to be about 25–30 m/s [*Ryan et al.*, 1981; see also *Ryan and Henry*, 1979]. (These estimated wind speeds of 25–30 m/s should be considered to be preliminary because they are based on analyses of partial data; the meteorology quadrant sensor failed on about Sol 45 and one of the two hot film anemometers failed on about Sol 376; peak gusts between Sols 45 and 376 were estimated to be 25.7 m/s and 25–30 m/s on Sol 423; current studies by J. E. Tillman of the University of Washington may resolve this problem.)

During the storm, the wind velocities at the height of the wind sensor most likely climbed rapidly to some value, say 40 m/s, producing wind friction speeds near 2.2–3.2 m/s (for surface roughness heights of 0.1–1.0 cm). Particles between about 20 μm and some larger size, related to particle density, would be set in motion. For 1.0 g/cm^3 clods, this upper size is 2–4.5 mm; for 2.0 g/cm^3 clods, it is 0.7–2.3 mm; and, for 3.0 g/cm^3 particles, it is 0.5–1.6 mm. Wind velocities of 50 m/s would produce wind friction speeds of 2.7–4.0 m/s (for roughness heights of 0.1–1.0 cm); in this case, particles between 10 μm and some larger size that is about twice those given above would be set in motion. The saltating clodlets and particles and suspended particles then erode the surface by impact and abrasion. In this process, particles much finer than the threshold size are produced—not only by impact with and abrasion of the surface, but also by disaggregation and abrasion of the impacting clodlets [e.g., *Sagan et al.*, 1977].

Erosion Rates

Erosion rates are difficult to establish, but it is clear that the erosion observed occurred within 29 sols. A minimum time to produce the observed erosion can be calculated using simplifying assumptions. According to White [e.g., equation (19), *White*, 1979], the amount of material with a uniform grain size that can be transported by aeolian saltation, suspension, and traction on a flat surface per unit width per unit time (q) is a function of the friction speed, the threshold friction speed required to saltate and entrain the particles, the density of the atmosphere, and the acceleration of gravity. Although Mars does not satisfy the conditions of a uniform grain size and a flat surface, White's equation suggests that the observed erosion could have taken place in a matter of a few to several tens of seconds. If it is assumed that a minimum particle size is set in motion with a threshold friction speed of 1.7 m/s and that the friction speed is 1.87 m/s, White's equation yields a value for q of 0.32 g/cm-s. The mass per unit width of pile 3 was about 13 g/cm. Thus one might conclude that pile 3 was removed in about 40 seconds. Smaller features, such as 1-cm-high trench tailings with masses per unit width values of 1 g/cm, would survive for about 3 seconds. This does not apply to pile 5 because most of the pile remained as a residue of coarse fragments.

Actual erosion rates were probably variable, but erosion occurred somewhere in between 29 sols and the few to several tens of seconds estimated in the calculations above. The poststorm surfaces are more akin to eroded surfaces of terrestrial soils that contain nonerodible elements such as clods and crusts [*Chepil*, 1945; *Chepil and Milne*, 1941; *Chepil and Woodruff*, 1963]. For terrestrial soils, erosion rates for undulating surfaces are smaller than for smooth planar ones. Erosion rates also decrease rapidly with time as more and more nonerodible elements are exhumed and exposed to the wind until the surface reaches an equilibrium condition. Similar variables related to surface configurations and material properties are illustrated by the conical piles. Pile 2, which was perched atop a rock, was removed, Pile 4, which was placed next to a rock, was partially eroded. Pile 3, which was placed among rocks, was removed except for a thin residue. Pile 5, which was placed among rocks, and the only one constructed with blocky material, was eroded to a broad mound composed of nonerodible fragments 0.7 cm and smaller. Thus the responses and erosion rates of all four of the piles during wind erosion in the same storm were different. Elsewhere, edges and rims of trenches in drift material were rounded and lumps were destroyed; in contrast, edges and rims of trenches in blocky material were stripped of fine materials leaving pebbly residues. In general, undisturbed materials were not eroded to a large degree. An exception to this is the exposed triangular face of drift material of the wind tail, which was rounded. Rocks were not detectibly eroded, although fines were removed from some of their surfaces. Thus the erosion rate of rocks was essentially zero. Finally, the observed erosion could be the cumulative effect of several erosional events.

Wind Directions

Wind directions inferred for the Dust Storm of Sol 1742 are more easterly than the paleo-wind directions inferred from the larger preexisting wind tails. The vector mean azimuth for the larger preexisting wind tails [*Sagan et al.*, 1977] is consistent with paleo-wind directions from 11.5° northeast. Wind directions inferred for the Sol 1742 storm are quite variable: miniature wind tails indicate N 30° E; erosion and movement of materials near the trenches in area J and the disrupted area in area F indicate about N 50° E; the triangular rock in area H indicates N 65° E; and pile 4 indicates a wind from the east. Such wide variations are probably related to local surface configurations that are out of equilibrium with respect to a northeasterly wind (at 1.6 m above the surface). Near-surface flow induced by a northeasterly wind blowing across a surface that has previously adjusted to northerly winds would be perturbed. The variety of unequilibrated configurations created by the lander and sampler would also perturb near surface flow.

One-tenth scale wind tunnel experiments might aid in establishing the direction of the eroding winds of the Sol 1742 storm. My best estimate from this study is N 52° E ± 23°.

CONCLUSIONS

1. Erosion during the storm occurred where the surface configurations and surface materials were in a condition of disequilibrium with respect to the stresses exerted by the wind and its entrained debris. Equilibrium configurations and physical states of the surface materials were altered by the lander, during landing and during sampler activities; the physical states of the bright dusts from global dust storms were in a natural condition of disequilibrium because the dusts were removed and redistributed by the storm and on previous occasions.

2. The various materials responded differently, depending on their configurations and physical states. Trench rims and other similar configurations of disturbed drift material were rounded; weak lumps and crusts were demolished. In contrast, fine

materials were stripped from trench rims and other similar configurations of disturbed blocky material so that pebbly residues were left behind; some clods were destroyed. Materials in markedly unequilibrated configurations, such as the conical piles, were demolished or substantially altered. Undisturbed materials in configurations and physical states that are apparently equilibrated to the Martian wind environment were not modified. Fine materials deposited from global dust storms, engine-exhaust gases, and the sampler were removed because of small cohesions and particle sizes. Large rocks were unaffected except for removal of fine materials from their surfaces.

3. Winds of the storm came from the northeast—probably about N 52° E. This direction differs significantly from the more northerly paleo-wind directions inferred from the large preexisting wind tails.

4. Winds probably attained speeds of about 40–50 m/s at a height of 1.6 m above the surface and friction speeds were probably about 2.2 to 4.0 m/s; a spectrum of particle sizes from ten or so microns and clods, up to 4–5 mm, were saltated by and entrained in the wind.

5. Erosion probably occurred within an interval somewhat larger than the few to several tens of seconds estimated with idealized models because the surfaces and materials of Mars are more akin to most terrestrial surfaces and soils where progressive exposures of nonerodible elements reduce erosion rates.

Acknowledgments. The author wishes to thank R. E. Arvidson, J. E. Tillman, and G. Ryder for their helpful reviews. Nathan Bridges, Gunn High School, Palo Alto, California, helped the author with the observations and measurements of changes produced by the Dust Storm of Sol 1742. This work was performed under NASA contract W15-462.

REFERENCES

Arvidson, R. E., E. A. Guinness, H. J. Moore, J. Tillman, and S. D. Wall, Three Mars years: Viking Lander 1 imaging observations, *Science, 222*, 463–468, 1983.

Bagnold, R. A., *The Physics of Blown Sand and Desert Dunes*, Methuen, London (reprinted 1965), 265 pp., 1941.

Chepil, W. S., Dynamics of wind erosion: I. Nature of movement of soil by wind, *Soil Sci., 60*, 305–320, 1945.

Chepil, W. S., and R. A. Milne, Wind erosion in relation to roughness of surface, *Soil Sci., 52*, 417–433, 1941.

Chepil, W. S., and N. P. Woodruff, The physics of wind erosion and its control, *Adv. Agron., 15*, 211–302, 1963.

Colburn, D. S., and J. B. Pollack, Mars aerosol observations during the second Viking year, *Eos Trans. AGU, 64*, 745, 1983.

Garvin, J. B., P. J. Mouginis-Mark, and J. W. Head, Characterization of rock populations on planetary surfaces: techniques and a preliminary analysis of Mars and Venus, *Moon and Planets, 24*, 355–387, 1981.

Guinness, E. A., C. E. Leiff, and R. E. Arvidson, Two Mars years of surface changes seen at the Viking landing sites, *J. Geophys. Res., 87*, 10,051–10,058, 1982.

Guinness, E. A., R. E. Arvidson, and H. J. Moore, Aeolian erosion and deposition seen on Mars from Mutch Memorial Station (Viking Lander 1), *Geol. Soc. Am. Abs. with Progs., 96th Annu. Mtg.*, 745, 1983.

Hess, S. L., J. A. Ryan, J. E. Tillman, R. M. Henry, and C. B. Leovy, The annual cycle of pressure on Mars measured by Viking Landers 1 and 2, *Geophys. Res. Lett., 7*, 197–200, 1980.

Hutton, R. E., H. J. Moore, R. F. Scott, R. W. Shorthill, and C. R. Spitzer, Surface erosion caused on Mars from the Viking descent engine plume, *Moon and Planets, 23*, 293–305, 1980.

Iversen, J. D., J. B. Pollack, R. Greeley, and B. R. White, Saltation threshold on Mars: The effect of interparticle forces, surfaces roughness, and low atmospheric density, *Icarus, 19*, 381–393, 1976*a*.

Iversen, J. D., R. Greeley, and J. B. Pollack, Wind blown dust on Earth, Mars, and Venus, *J. Atmos. Sci., 33*, 2425–2429, 1976*b*.

James, P. B., and N. Evans, A local dust storm in the Chryse region of Mars: Viking Orbiter observations, *Geophys. Res. Lett., 8*, 903–906, 1981.

Jones, K. L., R. E. Arvidson, E. A. Guinness, S. L. Bragg, S. D. Wall, C. E. Carlston, and D. G. Pidek, One Mars year: Viking Lander imaging observations, *Science, 204*, 799–806, 1979.

Leovy, C. B., Observations of martian tides over two annual cycles, *J. Atmos. Sci., 38*, 39–39, 1981.

Moore, H. J., Erosion of surface materials at the Mutch Memorial Station (Lander 1), Mars, *Repts. of Planet. Geol. Prog.*, pp. 180–181, NASA TM-85127, 1982.

Moore, H. J., Local dust storm of Sol 1742, Mars (abstract), in *Lunar and Planetary Science XVI*, pp. 572–573, Lunar and Planetary Institute, Houston, 1985*a*.

Moore, H. J., Observed changes at Viking Lander 1, *Repts. of Planet. Geol. Prog., 1984*, pp. 285–287, NASA TM-87563, 1985*b*.

Moore, H. J., and E. M. Dowey, Maps of the sample fields and summary of surface activities of Viking Lander 1 and 2, *Third International Colloquium on Mars*, 50 pp., Lunar and Planetary Institute, Houston, 1981.

Moore, H. J., R. E. Hutton, R. F. Scott, C. R. Spitzer, and R. W. Shorthill, Surface materials of the Viking landing sites, *J. Geophys. Res., 82*, 4497–4523, 1977.

Moore, H. J., C. R. Spitzer, K. Z. Bradford, P. M. Cates, R. E. Hutton, and R. W. Shorthill, Sample fields of the Viking landers, physical properties, and aeolian processes, *J. Geophys. Res., 84*, 8365–8377, 1979.

Moore, H. J., G. D. Clow, and R. E. Hutton, A summary of Viking sample trench analyses for angles of internal friction and cohesions, *J. Geophys. Res., 87*, 10,043–10,050, 1982.

Moore, H. J., E. A. Guinness, and R. E. Arvidson, Dust storms witnessed by Viking Lander 1, Mars, *Eos Trans. AGU, 64*, 745, 1983.

Ryan, J. A., and R. M. Henry, Mars atmospheric phenomena during major dust storms, as measured at the surface, *J. Geophys. Res., 84*, 2821–2829, 1979.

Ryan, J. A., and R. D. Sharman, Two major dust storms one year apart: comparison from Viking data, *J. Geophys. Res., 86*, 3247–3257, 1981.

Ryan, J. A., R. D. Sharman, and R. D. Lucich, Local Mars dust storm generation mechanism, *Geophys. Res. Lett., 8*, 899–901, 1981.

Sagan, C., D. Pieri, P. Fox, R. E. Arvidson, and E. A. Guinness, Particle motion on Mars inferred from the Viking Lander cameras, *J. Geophys. Res., 82*, 4430–4438, 1977.

Sharp, R. P., and M. C. Malin, Surface geology from Viking landers on Mars: a second look, *Geol. Soc. Am. Bull., 95*, 1398–1412, 1984.

Sutton, J. L., C. B. Leovy, and J. E. Tillman, Diurnal variations of the martian surface layer meteorological parameters during the first 45 sols at the two Viking Lander sites, *J. Atmos. Sci., 35*, 2346–2355, 1978.

Tillman, J. E. Dynamics of the boundary layer of Mars, *Proceedings of the Symposium on Planetary Atmospheres*, pp. 145–149, Royal Society of Canada, Ottawa, 1977.

Tillman, J. E., Martian meteorology and dust storms from Viking observations, *Proceedings of the Conference on the Case for Mars II*, Am. Astron. Soc., 1985, in press.

Tillman, J. E., R. M. Henry, and S. L. Hess, Frontal systems during passage of the north polar hood over the Viking Lander 2 site prior to the first 1977 dust storm, *J. Geophys. Res., 84*, 2947–2955, 1979.

Wall, S. D., Viking Lander monitor mission imaging investigation status report, *Repts. of Planet. Geol. Prog.*, pp. 379–381, NASA TM-85127, 1982.

Wall, S. D., and T. C. Ashmore, Conclusions of Viking Lander imaging investigation, *NASA Ref. Pub. 1137*, 202 pp., 1985.

White, B. R., Soil transport by winds on Mars, *J. Geophys. Res., 84*, 4643–4651, 1979.

H. J. Moore, Branch of Astrogeologic Studies, U.S. Geological Survey, MS946, 345 Middlefield Road, Menlo Park, Ca 94025.

(Received April 30, 1985;
revised August 13, 1985;
accepted August 19, 1985.)